TU Delft

Challenging Glass 2 – Conference on Architectural and Structural Applications of Glass,
Bos, Louter, Veer (Eds.), TU Delft, May 2010.
Copyright © with the authors. All rights reserved.

Structural Glass Beams with Embedded Glass Fibre Reinforcement

Christian Louter
Faculty of Architecture, TU Delft, The Netherlands / ICOM, EPFL, Switzerland
p.c.louter@tudelft.nl, www.glass.bk.tudelft.nl, http://icom.epfl.ch
Calvin Leung, Henk Kolstein, Jan Vamberský
Faculty of Civil Engineering & Geosciences, TU Delft, The Netherlands

This paper investigates the possibilities of pultruded glass fibre rods as embedded reinforcement in SentryGlas (SG) laminated glass beams. To do so, a series of pull-out tests, to investigate the bond strength of the rods to the laminate, and a series of beam tests, to investigate the post-breakage response of the beams, have been performed. Both test series have been conducted for round E-glass fibre rods and flat S-glass fibre rods. The pull-out tests showed superior pull-out strength of the flat rods, due to their large bond area. Furthermore, the beam tests showed superior post-breakage performance of the beams with the flat rods, due to higher strength and stiffness of the S-glass fibres. Overall, it is concluded that embedding glass fibre reinforcement in a SG-laminated glass beam is a very promising concept.

Keywords: reinforcement, embedded, glass fibre, laminate, interlayer, beam

1. General

In addition to the ongoing research at Delft University of Technology (TU Delft) on metal reinforced glass beams [1], current study focuses on a novel concept of glass fibre reinforcement rods embedded in the interlayer of laminated structural glass beams. The purpose of the glass fibre reinforcement is to increase the redundancy of the glass beams and to generate a high post-breakage strength upon and after possible glass failure.

The glass fibre reinforcement rods provide some advantages over a metal reinforcement section. Firstly, due to the semi-transparent appearance of the glass fibre rods the overall transparency of the reinforced glass beam is increased. Secondly, due to the high tensile strength of the glass fibres the amount of reinforcement needed within the beam laminate is limited, which will even further enhance the transparency of the beam. However, a disadvantage of the glass fibre rods might be that the glass fibres, unlike the ductile metal reinforcement, fail in a brittle manner. To some extent, this might endanger the redundancy of the glass fibre reinforced glass beams.

To host the glass fibre reinforcement rods, the polymer interlayer material SentryGlas (SG) seems a promising candidate. This interlayer material, which has originally been developed by DuPont for hurricane, vandalism and burglary resistant glazing, offers relatively high shear stiffness [2] and significant bond strength [3, 4] and has successfully been applied as a bond between metal reinforcement and glass in preceding research [5]. Furthermore, due to its high flow characteristics when heated during the

lamination process, the SG interlayer is expected to easily adapt to the geometry of the glass fibre reinforcement rods embedded in the interlayer.

To validate the concept of glass fibre reinforcement embedded in the interlayer of structural glass beams, two different beam designs containing either round or flat glass fibre reinforcement rods, have been produced and tested in four-point bending. Additionally, small pull-out specimens have been made and loaded in tension to investigate the bond strength of both the round and flat glass fibre rods to the laminate. To simultaneously investigate the effect of temperature on the bond strength, the pull-out tests have been performed at -20, 23 and 60°C. This paper forms an extension to the preliminary results of bending tests performed on glass beams with embedded glass fibre reinforcement rods presented by Louter [6] at the GPD 2009 conference.

2. Test specimens

The number of specimens produced and tested in this research is provided in Table 1. The following sections discuss the materials and geometry used for the specimens.

Table 1: Overview of number of test specimens per test type.

Test condition	Pre-conditioning	Pull-out specimens		Beam specimens	
		round rods	flat rods	round rods	flat rods
-20°C	1 week at -23°C	2	2	n/a	n/a
23°C	1 week at 23°C	2	3	2	2
60°C	24 hours at 63°C	2	3	n/a	n/a

2.1. Materials

Both the pull-out and beam specimens have been composed of glass, SG interlayer sheets and pultruded glass fibre rods. Their main properties are listed in Table 2 and 3. Ordinary annealed float glass, with ground edges, has been applied for all specimens. Sheets with standard thicknesses of 1.52 and 0.9 mm have been applied for the SG interlayer. Since it is expected to enhance the bond strength, all specimens have been laminated with the tin side of the glass facing inwards, towards the glass fibre reinforcement rods.

Two different types of pultruded glass fibre rods, round and flat, have been applied within this research. These glass fibre rods, which are normally applied within composite structures like car and aeroplane bodyworks, consist of glass fibre filaments embedded in a resin matrix. The round rods, with a diameter of 2 mm, consist of E-glass fibre filaments embedded in a polyester matrix. The flat rods with section dimensions of 0.8 x 6 mm, consist of S-glass fibre filaments embedded in an epoxy resin. The amount of glass fibre filaments within the resin matrix is expressed by the volume fraction, see Table 3. Due to handling of the glass fibre filaments during the process of bundling, the glass fibres loose about 25% of their virgin filament strength [7]. The strength of the round rods is therefore estimated at $0.75 \times \sigma_{fil} \times v_{rod} \times A_{rod} = 0.75 \times 3400 \times 0.63 \times 3.1 = 5.0$ kN and at $0.75 \times \sigma_{fil} \times v_{rod} \times A_{rod} = 0.75 \times 4600 \times 0.65 \times 4.8 = 10.8$ kN for the flat rods. The contribution of the matrices to the overall tensile strength has been neglected in this calculation.

Table 2: Material properties of annealed glass [8] and SentryGlas interlayer material [2, 9].

Property	Unit	Material	
		Glass, annealed	Interlayer, SentryGlas
Tensile strength	MPa	45	at 20°C: 34.5
Elastic modulus	MPa	70 x10^3	at 20°C*: 493; at 60°C*: 5.10
Shear modulus	MPa		at 20°C*: 169; at 60°C*: 1.70
Glass transition temperature	°C	n/a	~ 55
Elongation at tear	%	-	400
Density	kg/m^3	2500	950
Coefficient of thermal expansion	1/K	9 x10^{-6} (20 – 300°C)	10 – 15 x10^{-3}

*for a load duration of one hour according to [2]

Table 3: Main properties of the round and flat pultruded glass fibre rods, [10, 11].

Geometry pultruded rod	Symbol	Unit	round	flat
Cross section dimensions	-	[mm]	ø 2	0.8 x 6
Cross sectional area	A_{rod}	[mm^2]	3.1	4.8
Volume fraction	v_{rod}	[%]	63	60 - 65
Glass fibre filaments			E-glass	S-glass
Tensile strength (virgin strength)	σ_{fil}	MPa	3400	4600
E-modulus	-	MPa	73 x10^3	83 – 90 x10^3

2.2. Pull-out specimens

The pull-out specimens consist of two small double-layered glass laminates with a glass fibre rod embedded in the interlayer, see Figure 1. The glass laminates are composed of two 100x100 mm glass plates with a thickness of 10 mm. For the specimens with the round glass fibre rods three layers of SG have been applied of which the middle layer has been cut to host the glass fibre rod, see Figure 1. For the specimens with the flat glass fibre rods only two SG layers have been applied, see Figure 1.

2.3. Beam specimens

The beam specimens, with a length of 1.5 m, consist of a double-layer glass laminate with either 5 round or 3 flat glass fibre reinforcement rods embedded in the SG interlayer, see Figure 1. For each beam specimen three SG interlayer sheets have been applied. The middle sheet has been cut to host the glass fibre rods and to keep the glass fibre rods at the correct position during the lamination process. Any differences in thickness between the rods and the SG have been leveled due to the high flow characteristics of the SG when heated during the lamination process.

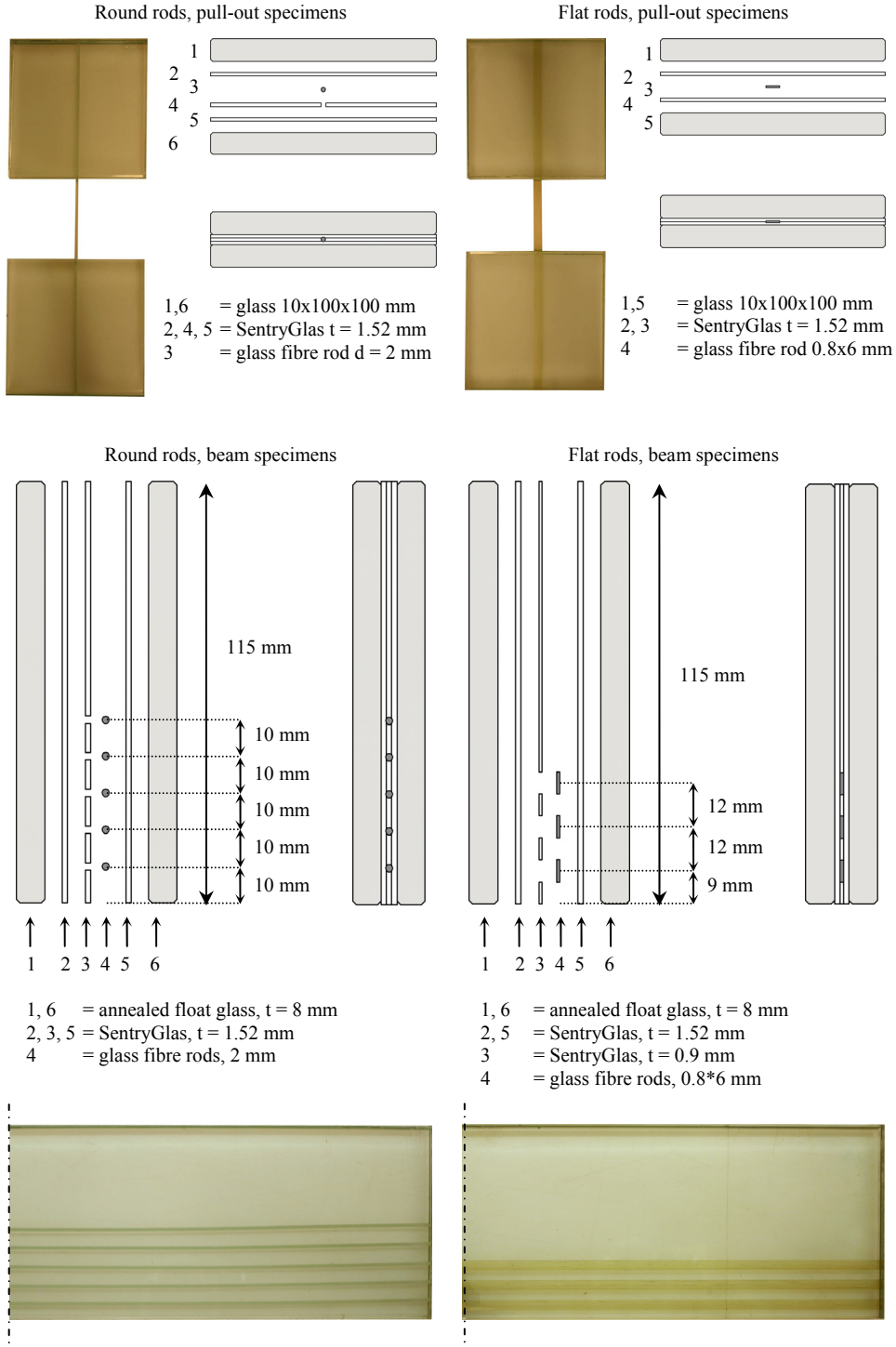

Figure 1: Exploded and assembled cross-sections and photographs of the pull-out and beam specimens.

3. Test setup

3.1. Pull-out tests

The pull-out tests at -20, 23 and 60°C have been performed on a standard Zwick Universal 100 kN testing machine at the Faculty of Mechanical, Maritime and Materials Engineering (TU Delft). The testing machine has been provided with steel brackets, which have been specially designed and custom-made for this research, to host the pull-out specimens, see Figure 2a. One part of the pull-out specimens has been placed in the upper bracket and the other part in the lower bracket. Subsequently, the upper bracket has been moved upwards at a constant displacement rate of 2 mm/minute, whereas the lower bracket was fixed. This way the glass fibre rod has been loaded in tension thereby pulling it out of the glass laminate.

For the pull-out tests at -20 and 60°C an insulated climatic box has been put around the test setup. During the tests the air inside the climatic box has been cooled or heated to -20 and 60°C respectively. Prior to the pull-out tests the specimens have been conditioned for several days at their test temperature plus an additional 3°C to compensate for any heat gain or loss during the mounting of the test specimens in the test setup, see Table 1.

3.2. Bending tests

The beam specimens have been tested in four-point bending at the Stevin Laboratory within the Faculty of Civil Engineering & Geosciences (TU Delft) on a standard testing machine which has been provided with a specially designed support frame. The support, load and lateral support span corresponded to the values shown in Figure 2b. The beams have been loaded until initial failure at a vertical displacement rate of 1 mm/min. Subsequently, the displacement rate has been increased stepwise to 2 and 5 mm/min. During all bending tests the inflicted load and the vertical displacement of the cross head, see Figure 2b, have been measured. The beam tests have been conducted at 23°C.

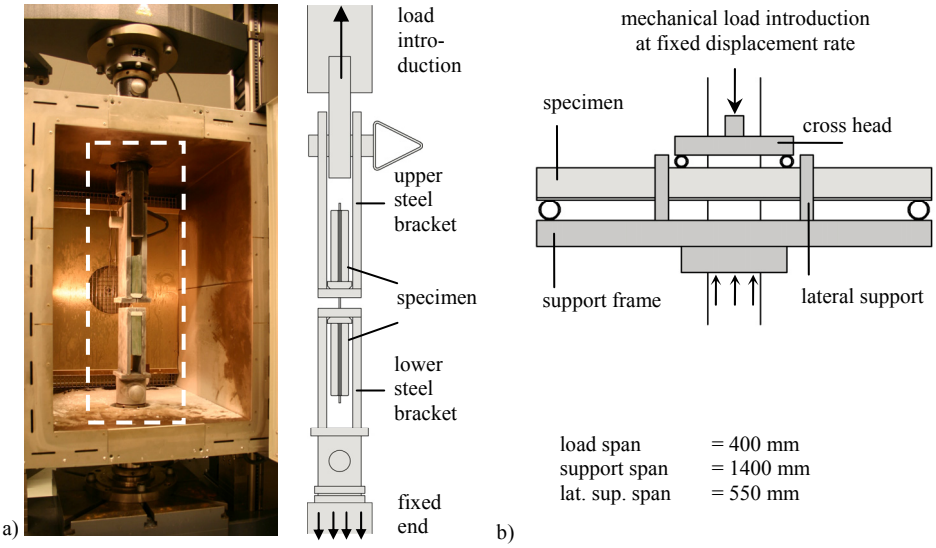

Figure 2: Test setup for the pull-out tests (left) and beam tests (right).

4. Test results

4.1. Pull-out tests

The results of the pull-out tests at -20, 23 and 60°C are presented in Table 4 and Figure 3. Generally, the pull-out specimens showed a capacity of carrying increasing loads until bond failure occurred, which caused a drop in load. For some pull-out specimens a residual pull-out resistance remained, which either gradually dropped or caused a hysteresis effect in the load-displacement diagram. Only for the specimens with the flat rods, tested at -20°C, full failure of the glass fibre rods occurred.

Table 4: Numerical results of the pull-out tests.

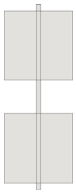

Maximum load		Round			Flat		
		-20°C	23°C	60°C	-20°C	23°C	60°C
mean	kN	3.0	3.2	2.3	10.7	9.1	8.0
st.dev	kN	0.1	0.0	0.1	0.0	0.6	1.4
rel.st.dev.	%	4.4	1.5	4.9	0.0	6.6	17.3

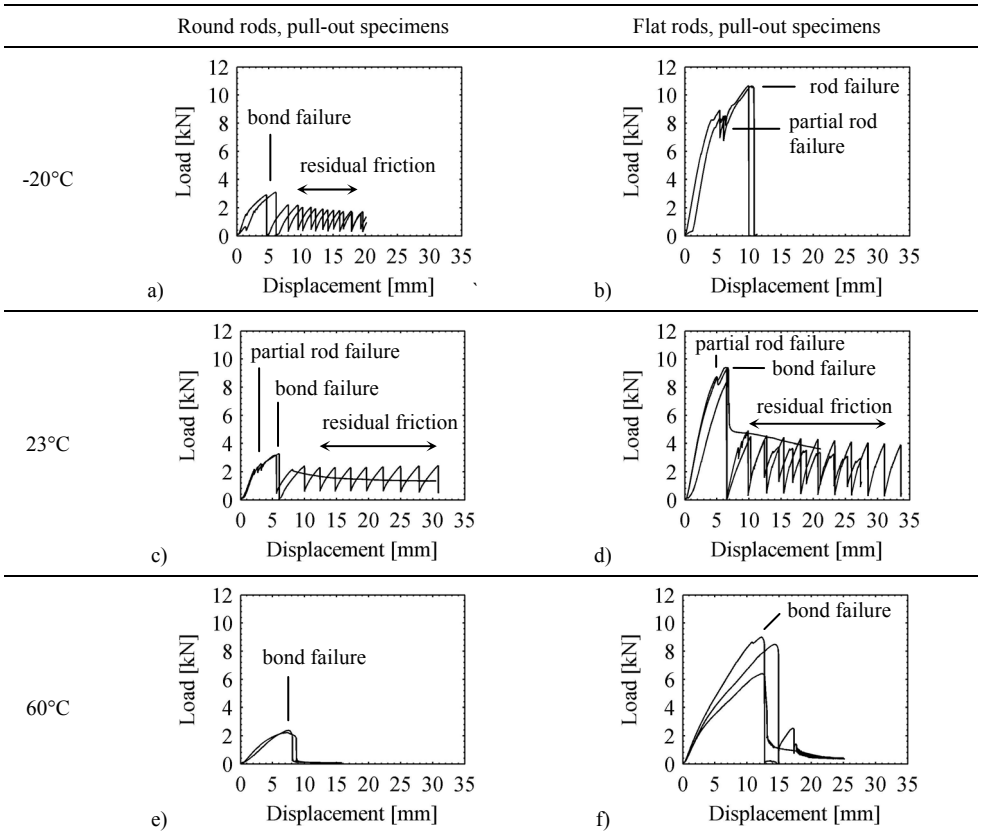

Figure 3: Load-displacement diagrams of the pull-out tests.

4.2. Bending tests

The results of the beam tests are presented in Table 5 and Figure 4. The latter provides the load-displacement diagrams and a schematic representation of the cracking sequence numbered a-d, which correlates to the letters in the diagrams. The beams showed linear elastic response until initial glass failure occurred in only one of the two glass sheets. After a drop in load, the load increased again and additional cracks occurred, see stage b. As loading was continued the cracks gradually started to propagate and typical diagonal shear cracks between the load and support points occurred, see stage c. At the end of the loading procedure the cracks in the beams were more or less evenly divided along the beam. For the beams with the round glass fibre reinforcement rods the tests had to be stopped at a displacement level of about 60 to 70 mm. At this stage the ultimate displacement capacity of the test setup had been reached, see stage d. For the beams with the flat glass fibre reinforcement rods, the test setup had been adapted to enlarge the displacement range. Those beams ultimately failed due to explosive glass failure. Mainly at the tensile edge the glass had detached from the laminate, see stage d.

Table 5: Numerical results of the beam tests.

	Round rods, pull-out specimens			Flat rods, pull-out specimens		
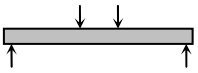	Initial failure load	Max. post breakage load	Post-breakage/ initial load	Initial failure load	Max. post breakage load	Post-breakage/ initial load
Mean	6.8 kN	7.8 kN	118.8 %	5.5 kN	11.6 kN	212.8 %
St. dev.	1.5 kN	0.1 kN	28.1 %	0.8 kN	0.5 kN	37.7 %
Rel. st .dev.	22.2 %	1.4 %	23.6 %	13.8 %	4.0 %	17.7 %

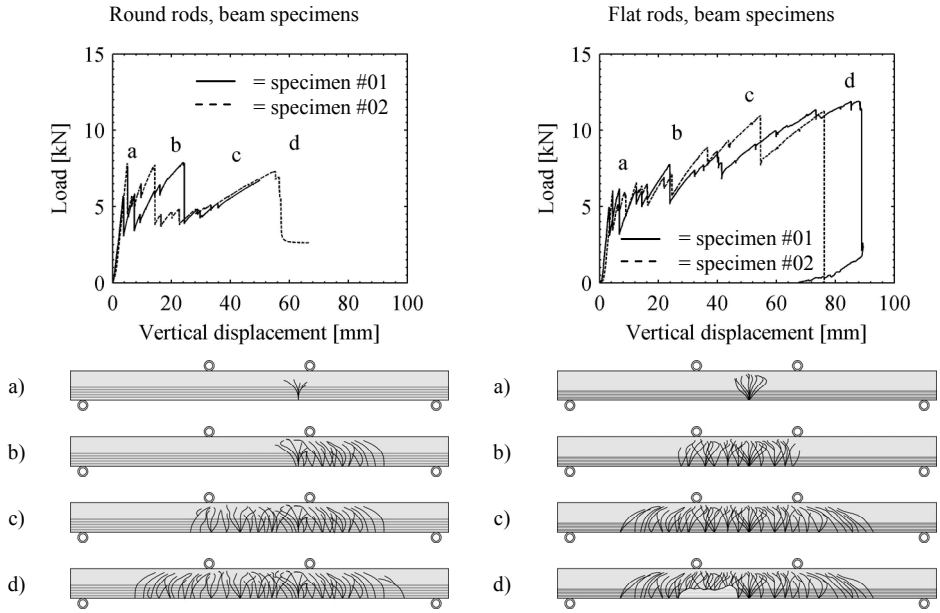

Figure 4: Load-displacement diagrams (up) and cracking sequence (below) of the beam specimens.

5. Discussion

5.1. Pull-out tests

The pull-out strength of the specimens with the flat glass fibre rods was, at all test temperatures, superior to the pull-out strength of the specimens with the round glass fibre rods, see Figure 5. This difference in pull-out strength is directly related to the difference in bond area of the round and flat glass fibre rods. Due to a larger outer surface of the flat rods, the shear transfer area of the flat rods is higher than for the round rods. As a result, the shear transfer capacity and consequent pull-out strength is larger for the flat rods. Additionally, the difference in pull-out strength might have, to some extent, also been caused by a difference in bond strength of the SG interlayer to the polyester and epoxy resin matrix applied for the round and the flat rods respectively. However, this possible difference in bond strength can not be derived from the tests performed within this research and requires additional testing.

The observed difference in pull-out strength at the different test temperatures, see Figure 5, is largely explained by a difference in shear stiffness of the SG interlayer at -20, 23 and 60°C. At the reference temperature 23°C, see Figure 5, the pull-out strength was relatively high for both the round and flat rods, due to a relatively high polymer stiffness and shear modulus of the SG at this temperature level, see Table 2. However, at 60°C the pull-out strength of both the round and flat specimens was significantly reduced, due to a decrease in shear stiffness of the SG interlayer at and above its glass transition temperature of ~55°C, see Table 2. At -20°C the pull-out strength of the specimens with the flat rods increased compared to 23°C, whereas it slightly decreased for the specimens with the round rods. The tendency of increasing pull-out strength at lower temperature levels, which has also been observed for metal inserted pull-out specimens [4], is in line with an increased shear stiffness of the SG interlayer at lower temperatures. However, the decrease in pull-out strength of the round specimens tested at -20°C does not fit this line of reasoning and no specific explanation for this decrease in pull-out strength of the round specimens at -20°C has been found. Though, it should be noted that the number of specimens was very small. Additional testing will be necessary to confirm the decrease in pull-out strength of the round specimens at -20°C.

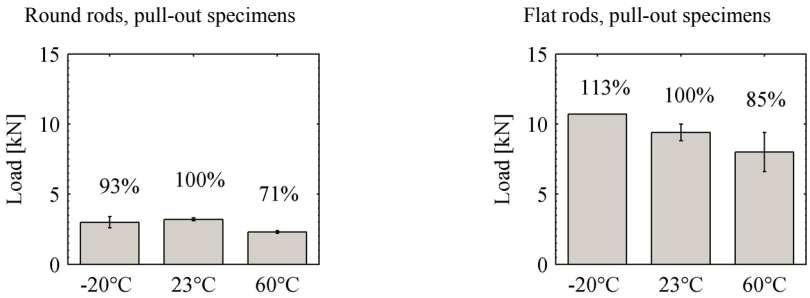

Figure 5: Bar graph of the mean pull-out strength values relative to the reference temperature 23°C.

5.1.1. Beam tests

Overall, the post-breakage performance of the beams with the flat rods was superior to the performance of the beams with the round rods. The beams with the flat rods showed

higher post-breakage strength and stiffness than the beams with the round rods, see Figure 4. This difference in post-breakage performance is explained by three aspects. Firstly, the total tensile capacity of the three flat reinforcement rods is, despite their smaller total cross-sectional area, higher than the total tensile capacity of the five round reinforcement rods. The smaller total cross-sectional area of the three flat rods is counteracted by the higher tensile strength of the S-glass fibre filaments in the flat rods compared to the E-glass fibre filaments in the round rods, see Table 3. The total tensile capacity of the five round reinforcement rods amounts 5 x 5.0 = 25.2 kN, whereas it amounts 3 x 10.8 = 32.3 kN for the three flat reinforcement rods. This large tensile capacity of the three flat rods results in a high bending moment capacity of the beams at the post-breakage stage. Secondly, the E-modulus of the S-glass fibres is higher than the E-modulus of the E-glass fibres which increases the post-breakage stiffness of the beam. Finally, the flat rods are positioned more towards the tensile edge of the beam than the round rods, see Figure 1. This increases the internal lever arm between tensile and compressive force within the beam, which effectively increases its bending moment capacity at the post-breakage stage.

Furthermore, a difference in failure mode between the beam types occurred. Whereas the beams with the round rods showed low beam stiffness at the post-breakage stage and, as they reached the ultimate deformation capacity of the test setup, could not be tested to full destruction, the beams with the flat rods showed high post-breakage stiffness and explosive final failure. Mainly at the tensile edge, but to some extent also at the compressive edge, the glass suddenly detached from the beam laminate. This caused a sudden collapse of the beam laminate and, despite lateral buckling supports, even full buckling of the beam laminate, see Figure 6. Although explosive glass failure has been observed before at the compression zone of reinforced glass beams [1] it has not been observed before at the tensile zone. It is assumed that the explosive detachment of glass at the tensile zone is most likely the result of a combined action of high stress in the glass, due to the high post-breakage loads, and a very large deformation of the beam laminate, which amounted about 65 to 80% of the beam height. This combined action of high stress and large deformation seemed to catapult the glass from the beam laminate.

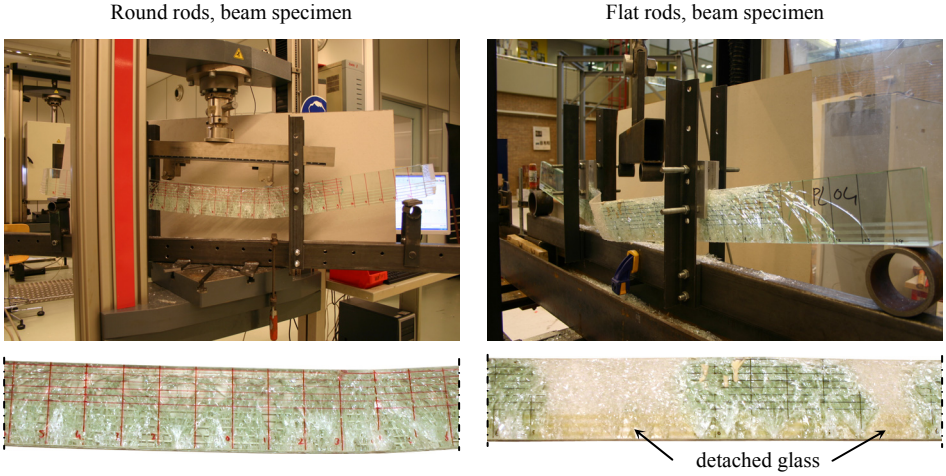

Figure 6: Tested beam specimen with round rods (left) and flat rods (right).

6. Conclusions

From the pull-out tests performed at -20, 23 and 60°C on small glass laminates with a round or flat pultruded glass fibre rod embedded in the SG interlayer, it is concluded that the pull-out strength of the specimens with flat rods is superior to the pull-out strength of the specimens with round rods. At all temperatures the specimens with the flat rods showed higher pull-out strength values. This superior performance is mainly the result of the larger bond area of the flat specimens compared to the round specimens.

From the bending tests performed on laminated glass beams with either round or flat pultruded glass fibre rods embedded in the SG interlayer, it is concluded that the post-breakage performance of the beams with the flat rods is superior to the performance of the beams with the round rods. Due to the higher strength and stiffness of the S-glass fibre filaments in the flat rods compared to the E-glass fibre filaments in the round rods, the total tensile capacity of the 3 flat rods applied per beam was higher than the total tensile capacity of the 5 round rods applied per beam. This effectively enhanced both the post-breakage strength and stiffness of the beams with the flat glass fibre rods.

Overall, it is concluded that embedding glass fibre rods in SG-laminated glass beams is a very promising concept, which provides highly redundant post-breakage beam response. Although the glass fibre reinforcement rods are brittle, the beam composites show 'ductile' post-breakage response and significant post-breakage strength. Their favourable structural performance combined with their highly transparent appearance make the beams appealing for structural and architectural applications.

Acknowledgements

The authors gratefully acknowledge the material support of glass supplier Van Noordenne Groep and interlayer manufacturer DuPont de Nemours. Additionally, Saint-Gobain and DPP Pultrusions are acknowledged for providing the flat glass fibre rods. Furthermore, the support of the Stevin Laboratory (CitG) and Materials Laboratory (3ME) of the TU Delft is acknowledged. Finally, the technical support of Björn Sanden, Joris Bohets, Jan de Loose and Yvan van Geenhoven is highly appreciated.

7. References

[1] Louter, Christian, *Adhesively Bonded Reinforced Glass Beams*, Heron, 52, 2007, http://heron.tudelft.nl
[2] Stelzer I, Bennison SJ. *SentryGlas, High-Performance Laminated Glass for Structurally Efficient Glazing*, Conference Proceedings Challenging Glass 2. Delft, 2010, www.bk.tudelft.nl/challengingglass
[3] Belis J, De Visscher K, Callewaert D, Van Imper R., *Laminating metal-to-glass: preliminary results of case-study*, In: Conference Proceedings GPD 2009, Finland; 2009, 191-193, www.glassfiles.com
[4] Louter, Christian, *Metal-to-glass bonding properties of an acrylate adhesive and SentryGlas at 23, -20 and 60°C*, Proceedings of the GPD 2009, Tampere, Finland, June 2009, www.glassfiles.com
[5] Louter, Christian; Bos, Freek; Callewaert, Dieter, Veer, Fred., *Performance of SentryGlas-laminated metal-reinforced glass beams at 23, -20 and 60°C,* GPD 2009, Finland, 2009, www.glassfiles.com
[6] Louter, PC, *High-strength fibre rods as embedded reinforcement in SentryGlas-laminated glass beams*, In the Proceedings of the Glass Performance Days 2009, Tampere, Finland, www.glassfiles.com
[7] Hartman D.R., Greenwood M.E., Miller D.M., *High Strength Glass Fibers*, Owens-Corning, 1998
[8] NEN-EN 572-1, *Glas voor gebouwen – Basisproducten van natronkalkglas – Deel 1: Definities en algemene fysische en mechanische eigenschappen*, Delft, The Netherlands, 2004
[9] Delince Didier, Callewaert, Dieter, Belis, Jan, Impe, Rudy Van, *Post-breakage Behaviour of Laminated Glass in Structural Applications*, Challenging Glass 1, Delft, 2008, www.bk.tudelft.nl/challengingglass
[10] R&G, *Chapter 08: Glass, aramid and carbon fibre*, R&G composite handbook edition 8, www.r-g.de
[11] TOHO TENAX EUROPE GmbH, *Datasheet Tenax HT5131*, www.tohotenax-eu.com